Basis Set and Electron Correlation Effects on Lithium Carbenoid Dimerization Energies

Lawrence M. Pratt,*[1] **Diep Huong Tran Phan,**[2] **Phuong Thao Thi Tran,**[2] **and Ngan Van Nguyen**[2]

[1]Department of Chemistry, Fisk University, 1000 17th Ave. N., Nashville, TN 37209, U.S.A.

[2]University of Pedagogy, 280 An Duong Vuong, District 5, Ho Chi Minh, Vietnam

Received November 13, 2006; E-mail: lpratt@fisk.edu

A systematic investigation was performed to determine which levels of theory are required to obtain accurate geometries and dimerization energies for lithium carbenoids. Dimerization free energies of six lithium carbenoids were calculated in the gas phase at the B3LYP and MP2 levels with several different basis sets and at the CCSD(T) level with the aug-cc-pvdz basis set. It was found that the calculated thermal corrections to the dimerization free energy, obtained from frequency calculation, were relatively independent of the basis set for basis sets larger than 6-31+G(d) and that smaller basis sets often generated qualitatively correct results. The dimerization free energies were usually overestimated by small basis sets compared to those using polarization and diffuse functions, whereas only modest gains were obtained by using basis sets larger than 6-31+G(d). The B3LYP DFT method generated geometries consistent with the MP2 and CCSD methods for halomethyllithium carbenoids, but not always for 1-halovinyllithium carbenoids. The B3LYP calculations also severely underestimated the dimerization free energies for the halovinyllithium carbenoids, compared to the MP2, and coupled cluster methods.

Organolithium compounds are among the most important reagents for carbon–carbon bond-forming reactions in organic chemistry and have been the subject of numerous theoretical investigations. In the 1980's, Schleyer and others investigated unusual bonding types in alkyllithiums and related species at low levels of theory.[1–4] Those results are more than a curiosity, as later experimental studies have confirmed that organolithium compounds form aggregates with non-classical bonding. In the 1990's, Collum and co-workers have published a series of papers using the MNDO semiempirical method to understand the structure of lithium dialkylamides.[5–8] Those studies are the product of good science and good fortune, as semiempirical methods work particularly well for lithium dialkylamides compared to other organolithium compounds. The availability of density functional theory (DFT) methods in commercial quantum chemistry programs by the late 1990's has rendered the NDDO semiempirical methods obsolete for most organolithium studies, and DFT methods are the mainstay of computational studies of organolithium compounds today. DFT methods are imperfect; however, they are referred to by some as "semiempirical quantum chemistry done right." In particular, DFT methods often generate very low activation energies for organolithium reactions, and occasionally fail to locate a barrier at all.[9,10] DFT methods still remain popular for calculation of activation barriers of organolithium species, largely because of the difficulty in performing high level ab initio calculations on large solvated molecules.[11–13] From the early studies of the 1980's to present, computational organic chemistry groups have generally performed calculations at the highest level that is practical for the system of interest. To the best of our knowledge, a systematic examination of the level of theory and basis set required to obtain chemical accuracy in lithium compounds has not yet been done. This report is an attempt to address this gap in the literature. Since reliable experimental determinations of the structural and thermochemical properties of families of organolithium compounds are rare, we focused on the gas-phase structures, for which large basis set MP2 and coupled cluster calculations can be performed at a reasonable computational cost.

Of particular interest is the structure and reactions of lithium carbenoids and related species. From our prior work, like other lithium compounds, they tend to form both homo and mixed aggregates.[14–17] Close examination of the geometries obtained with different basis sets also led us to suspect that lithium carbenoids and carbenoid-like species may have relatively flat potential energy surfaces and therefore may be particularly sensitive to basis set and electron correlation effects. Those suspicions turned out to be correct, particularly for 1-halovinyllithium carbenoids, as described in detail below.

This paper seeks to answer several questions with regard to basis sets and electron correlation methods. First, what level of theory is necessary to obtain good geometries for single point energy calculations at higher levels of theory? Will DFT do the job, or are more expensive MP2 or CCSD optimizations required? Secondly, what level is required to obtain accurate dimerization energies? The final issue is the calculation of thermodynamic corrections to the free energy, obtained by frequency calculations. At high levels of theory those can be prohibitively expensive, particularly for large molecules. Can satisfactory thermal corrections be obtained at lower levels of theory and be added to electronic-nuclear repulsion energies calculated at higher levels?

Published on the web August 10, 2007; doi:10.1246/bcsj.80.1587

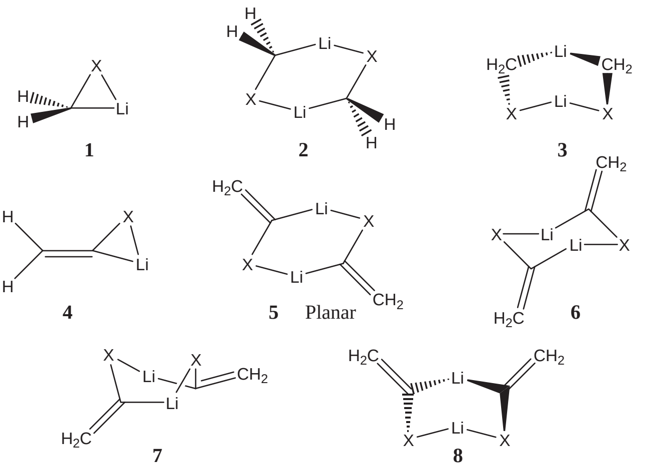

Chart 1.

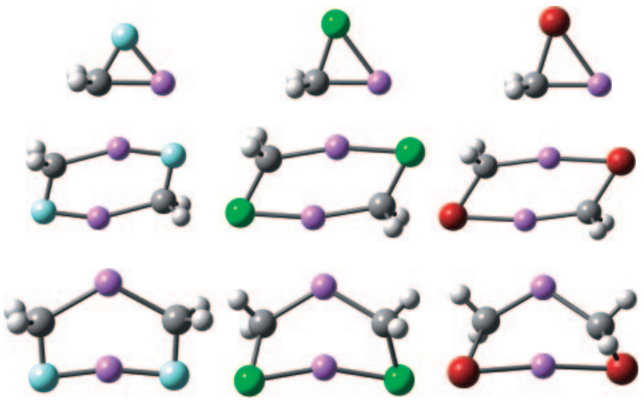

Fig. 1. Optimized geometries of halomethyllithium carbenoids. Top row: monomer **1**; Center row: dimer **2**; Bottom row: dimer **3**. Grey: carbon; white: hydrogen; light blue: fluorine; green: chlorine; red: bromine; violet: lithium.

Computational Methods

All geometry optimizations and frequency calculations were performed with the Gaussian 98 or Gaussian 03 programs.[18] The calculated thermal corrections to the free energies were unscaled. DFT calculations were performed with the B3LYP hybrid functional. Geometry optimizations and frequency calculations were performed with the MIDIX, 6-31G(d), 6-31+G(d), 6-31+G(d,p), 6-31++G(d,p), and 6-311++G(d,p) basis sets. Single point energies were calculated with the 6-311++G(df,pd), 6-311++G(2df,2pd), and 6-311++G(3df,3pd) basis sets, and the free energies were estimated using the thermal corrections calculated with the 6-311++G(d,p) basis set. MP2 single point energies, geometry optimizations, and frequency calculations were performed with the same basis sets. In addition, MP2 optimizations and frequencies were calculated with the aug-cc-pvdz and aug-cc-pvtz basis sets, and CCSD(T) single point energies were calculated with the aug-cc-pvdz basis set at the MP2/aug-cc-pvdz geometry. To verify the validity of the MP2 geometries, the geometries were also optimized at the CCSD/6-31+G(d) level.

Results and Discussion

Six lithium carbenoids were chosen for this study. Fluoro-, chloro-, and bromomethyllithiums were chosen as the simplest lithium carbenoids. In addition to the monomer **1**, we have previously reported a planar dimeric structure **2**,[14] and since then, a second dimeric structure **3** was found during a computational study of carbenoid reaction mechanisms. The remaining three carbenoids were 1-halovinyllithiums. These were of interest because preliminary work on the FBW rearrangement of these compounds suggested that the potential energy surface may be relatively flat. In addition to the monomer **4**, a previous DFT study found that the dimers optimized to a nearly, but not quite planar structure.[17] Therefore, for the dimer, planar **5**, chair **6**, and twist-boat **7** geometries, and an unsymmetrical dimer **8** were used as starting structures for the geometry optimizations (Chart 1).

Comparison of large basis set MP2 calculations with the CCSD(T) and G3 methods generally yielded similar dimerization energies, as shown below. Although it is difficult to say

Table 1. Optimized MP2 [B3LYP] Bond Lengths (Å) and Angles (degrees) for the Halomethyllithium Monomers **1**

Basis set	Molecule	C–Li	C–X	Li–X	θ C–Li–X
MIDIX	$LiCH_2F$	1.922	1.545	1.675	50.3
		[1.910]	[1.557]	[1.659]	[51.2]
6-31G(d)	$LiCH_2F$	1.946	1.565	1.760	49.7
		[1.923]	[1.576]	[1.737]	[50.7]
6-31+G(d)	$LiCH_2F$	1.952	1.585	1.799	49.8
		[1.927]	[1.599]	[1.772]	[51.0]
6-31++G(d,p)	$LiCH_2F$	1.952	1.583	1.798	49.7
		[1.929]	[1.601]	[1.769]	[51.1]
6-311++G(d,p)	$LiCH_2F$	1.933	1.560	1.793	49.3
		[1.919]	[1.602]	[1.764]	[51.3]
aug-cc-pvdz	$LiCH_2F$	1.958	1.592	1.791	50.0
aug-cc-pvtz	$LiCH_2F$	1.929	1.556	1.788	49.3
CCSD/6-31+G(d)	$LiCH_2F$	1.953	1.592	1.782	50.2
MIDIX	$LiCH_2Cl$	1.946	1.977	2.198	56.6
		[1.926]	[2.045]	[2.207]	[58.8]
6-31G(d)	$LiCH_2Cl$	1.972	1.909	2.287	52.6
		[1.946]	[1.993]	[2.268]	[55.8]
6-31+G(d)	$LiCH_2Cl$	1.977	1.910	2.270	52.9
		[1.951]	[1.994]	[2.266]	[55.8]
6-31++G(d,p)	$LiCH_2Cl$	1.976	1.908	2.272	52.8
		[1.951]	[1.995]	[2.262]	[55.9]
6-311++G(d,p)	$LiCH_2Cl$	1.955	1.904	2.207	54.0
		[1.939]	[1.996]	[2.215]	[56.9]
aug-cc-pvdz	$LiCH_2Cl$	1.989	1.942	2.294	53.3
aug-cc-pvtz	$LiCH_2Cl$	1.963	1.901	2.252	53.1
CCSD/6-31+G(d)	$LiCH_2Cl$	1.978	1.949	2.267	54.1
MIDIX	$LiCH_2Br$	1.962	2.157	2.394	58.4
		[1.932]	[2.183]	[2.353]	[60.3]
6-31G(d)	$LiCH_2Br$	1.988	2.093	2.392	56.2
		[1.956]	[2.145]	[2.352]	[58.9]
6-31+G(d)	$LiCH_2Br$	1.994	2.090	2.433	55.3
		[1.962]	[2.144]	[2.397]	[57.9]
6-31++G(d,p)	$LiCH_2Br$	1.995	2.086	2.434	55.1
		[1.964]	[2.141]	[2.396]	[57.8]
6-311++G(d,p)	$LiCH_2Br$	1.967	2.062	2.388	55.5
		[1.947]	[2.146]	[2.380]	[58.4]
aug-cc-pvdz	$LiCH_2Br$	1.996	2.077	2.457	54.4
aug-cc-pvtz	$LiCH_2Br$	1.970	2.036	2.400	54.5
CCSD/6-31+G(d)	$LiCH_2Br$	1.994	2.134	2.423	56.8

Table 2. Optimized MP2 [B3LYP] Bond Lengths (Å) and Angles (degrees) for the Halomethyllithium Dimers **2**

Basis set	Molecule	C–Li	C–X	Li–X	θ C–Li–X
MIDIX	LiCH$_2$F	2.142	1.512	1.708	157.4
		[2.112]	[1.520]	[1.698]	[158.5]
6-31G(d)	LiCH$_2$F	2.180	1.539	1.758	157.9
		[2.137]	[1.541]	[1.742]	[157.3]
6-31+G(d)	LiCH$_2$F	2.177	1.549	1.783	158.1
		[2.135]	[1.552]	[1.766	[157.8]
6-31++G(d,p)	LiCH$_2$F	2.174	1.546	1.784	157.6
		[2.133]	[1.553]	[1.766]	[157.6]
6-311++G(d,p)	LiCH$_2$F	2.162	1.523	1.793	158.0
		[2.139]	[1.550]	[1.775]	[158.6]
aug-cc-pvdz	LiCH$_2$F	2.182	1.552	1.793	157.6
aug-cc-pvtz	LiCH$_2$F	2.166	1.518	1.796	158.1
CCSD/6-31+G(d)	LiCH$_2$F	2.171	1.551	1.772	157.7
MIDIX	LiCH$_2$Cl	2.138	1.909	2.159	168.8
		[2.112]	[1.957]	[2.172]	[170.4]
6-31G(d)	LiCH$_2$Cl	2.144	1.872	2.235	166.6
		[2.146]	[1.929]	[2.239]	[168.2]
6-31+G(d)	LiCH$_2$Cl	2.144	1.872	2.235	166.6
		[2.135]	[1.928]	[2.233]	[168.2]
6-31++G(d,p)	LiCH$_2$Cl	2.142	1.870	2.234	166.2
		[2.135]	[1.929]	[2.232]	[168.1]
6-311++G(d,p)	LiCH$_2$Cl	2.147	1.869	2.197	158.5
		[2.147]	[1.930]	[2.210]	[169.1]
aug-cc-pvdz	LiCH$_2$Cl	2.179	1.899	2.272	158.1
aug-cc-pvtz	LiCH$_2$Cl	2.162	1.868	2.242	157.8
CCSD/6-31+G(d)	LiCH$_2$Cl	2.142	1.896	2.234	166.9
MIDIX	LiCH$_2$Br	2.153	2.087	2.352	172.2
		[2.119]	[2.010]	[2.327]	[173.2]
6-31G(d)	LiCH$_2$Br	2.170	2.054	2.341	170.8
		[2.139]	[2.091]	[2.316]	[172.0]
6-31+G(d)	LiCH$_2$Br	2.158	2.044	2.387	169.4
		[2.128]	[2.080]	[2.364]	[170.6]
6-31++G(d,p)	LiCH$_2$Br	2.151	2.039	2.391	168.5
		[2.125]	[2.077]	[2.367]	[169.9]
6-311++G(d,p)	LiCH$_2$Br	2.153	2.025	2.372	159.6
		[2.147]	[2.083]	[2.373]	[162.8]
aug-cc-pvdz	LiCH$_2$Br	2.172	2.039	2.431	152.8
aug-cc-pvtz	LiCH$_2$Br	2.153	2.004	2.381	157.2
CCSD/6-31+G(d)	LiCH$_2$Br	2.154	2.072	2.380	170.0

Table 3. Optimized MP2 [B3LYP] Bond Lengths (Å) and Angles (degrees) for the Halomethyllithium Dimers **3**

Basis set	Molecule	C–Li	C–X	Li–X	θ C–Li–C
MIDIX	LiCH$_2$F	2.125	1.511	1.710	120.7
		[2.090]	[1.521]	[1.700]	[121.1]
6-31G(d)	LiCH$_2$F	2.159	1.533	1.768	120.5
		[2.117]	[1.538]	[1.744]	[121.9]
6-31+G(d)	LiCH$_2$F	2.159	1.544	1.790	120.6
		[2.114]	[1.549]	[1.768]	[122.3]
6-31++G(d,p)	LiCH$_2$F	2.157	1.542	1.790	120.7
		[2.114]	[1.549]	[1.768]	[122.2]
6-311++G(d,p)	LiCH$_2$F	2.142	1.520	1.795	120.2
		[2.111]	[1.546]	[1.779]	[122.2]
aug-cc-pvdz	LiCH$_2$F	2.157	1.548	1.799	120.7
aug-cc-pvtz	LiCH$_2$F	2.140	1.515	1.799	119.8
CCSD/6-31+G(d)	LiCH$_2$F	2.154	1.547	1.779	121.1
MIDIX	LiCH$_2$Cl	2.111	1.907	2.174	125.0
		[2.074]	[1.954]	[2.199]	[124.1]
6-31G(d)	LiCH$_2$Cl	2.147	1.869	2.263	120.8
		[2.111]	[1.928]	[2.282]	[121.2]
6-31+G(d)	LiCH$_2$Cl	2.135	1.869	2.252	120.9
		[2.104]	[1.926]	[2.278]	[121.3]
6-31++G(d,p)	LiCH$_2$Cl	2.135	1.867	2.253	120.5
		[2.104]	[1.926]	[2.277]	[121.2]
6-311++G(d,p)	LiCH$_2$Cl	2.124	1.866	2.213	119.8
		[2.101]	[1.925]	[2.254]	[121.2]
aug-cc-pvdz	LiCH$_2$Cl	2.144	1.898	2.303	120.0
aug-cc-pvtz	LiCH$_2$Cl	2.126	1.867	2.274	119.4
CCSD/6-31+G(d)	LiCH$_2$Cl	2.130	1.891	2.254	121.3
MIDIX	LiCH$_2$Br	2.115	2.086	2.396	123.4
		[2.074]	[2.098]	[2.377]	[123.2]
6-31G(d)	LiCH$_2$Br	2.141	2.051	2.379	120.9
		[2.105]	[2.090]	[2.360]	[121.9]
6-31+G(d)	LiCH$_2$Br	2.123	2.049	2.414	119.6
		{2.093]	[2.087]	[2.404]	[120.5]
6-31++G(d,p)	LiCH$_2$Br	2.122	2.044	2.414	119.8
		[2.092]	[2.084]	[2.402]	[120.7]
6-311++G(d,p)	LiCH$_2$Br	2.122	2.023	2.403	119.8
		[2.096]	[2.081]	[2.430]	[120.8]
aug-cc-pvdz	LiCH$_2$Br	2.137	2.039	2.463	119.5
aug-cc-pvtz	LiCH$_2$Br	2.120	2.005	2.414	118.8
CCSD/6-31+G(d)	LiCH$_2$Br	2.118	2.077	2.409	120.2

that one of those methods is better than the others, the CCSD(T)/aug-cc-pvdz//MP2/aug-cc-pvdz energies were taken as the best available energies, to which all other calculations were compared. Although the G3, G3MP2, and G3B3 methods all yielded similar energies to the coupled cluster calculations, the geometries of the initial Hartree–Fock or B3LYP optimized structures were sometimes called into question, as shown in the subsequent discussion, and hence we chose the CCSD(T) method as the standard.

Basis Set Effects on Optimized Geometries. The MP2/6-31+G(d) optimized geometries of the halomethyllithium monomers and dimers are shown in Fig. 1. Starting with the MP2/6-31+G(d) optimized geometry and re-optimizing with successively larger basis sets through 6-311++G(d,p), each successive optimization required fewer than 5 optimization steps. The B3LYP geometries were similar to those obtained by MP2, and exhibited similar optimization behavior with larger basis sets. The smaller 6-31G(d) and MIDIX basis sets were used to reoptimize the 6-31+G(d) geometries at both the MP2 and B3LYP levels. The optimized bond lengths and angles using selected basis sets are given in Tables 1–3 for the monomer **1** and dimers **2** and **3**, respectively.

The optimized bond lengths with the 6-311++G(d,p) basis set were nearly identical to those obtained with the 6-31+(d) basis set for both the MP2 and B3LYP methods. Therefore, single point energies using more polarization and diffuse functions on 6-31+G(d) geometries should be nearly as good as the energies obtained by full geometry optimization with the larger basis sets, at a fraction of the cost in computer time. With each basis set, except the MIDIX, the bond lengths were within about 0.04 Å of each other, and the largest changes in bond lengths occurred upon going from a double zeta to a triple zeta basis set. For the halolithium monomers, the C–Li–X bond angles were within 2 degrees of each other with each

Table 4. Optimized MP2 [B3LYP] Bond Lengths (Å) and Angles (degrees) for the Halovinyllithium Monomers **4**

Basis set	Molecule	C–Li	C–X	Li–X	θ C–Li–X
MIDIX	CH_2=CLiF	1.918	1.535	1.688	49.9
		[1.890]	[1.551]	[1.669]	[51.2]
6-31G(d)	CH_2=CLiF	1.941	1.577	1.763	50.1
		[1.922]	[1.601]	[1.732]	[51.5]
6-31+G(d)	CH_2=CLiF	1.943	1.606	1.795	50.7
		[1.923]	[1.643]	[1.753]	[52.8]
6-31++G(d,p)	CH_2=CLiF	1.943	1.602	1.798	50.5
		[1.924]	[1.645]	[1.754]	[52.9]
6-311++G(d,p)	CH_2=CLiF	1.926	1.572	1.798	49.8
		[1.913]	[1.656]	[1.751]	[53.5]
aug-cc-pvdz	CH_2=CLiF	1.948	1.613	1.788	50.9
aug-cc-pvtz	CH_2=CLiF	1.922	1.562	1.800	49.5
CCSD/6-31+G(d)	CH_2=CLiF	1.945	1.625	1.770	50.7
MIDIX	CH_2=CLiCl	1.935	2.034	2.156	59.3
		[1.911]	[2.157]	[2.140]	[64.0]
6-31G(d)	CH_2=CLiCl	1.953	1.962	2.265	54.8
		[1.946]	[2.160]	[2.210]	[62.2]
6-31+G(d)	CH_2=CLiCl	1.953	1.955	2.266	54.6
		[1.946]	[2.160]	[2.210]	[62.3]
6-31++G(d,p)	CH_2=CLiCl	1.953	1.949	2.269	54.4
		[1.946]	[2.166]	[2.208]	[62.5]
6-311++G(d,p)	CH_2=CLiCl	1.937	1.941	2.217	55.2
		[1.929]	[2.166]	[2.173]	[63.4]
aug-cc-pvdz	CH_2=CLiCl	1.964	1.982	2.300	54.7
aug-cc-pvtz	CH_2=CLiCl	1.941	1.940	2.259	54.4
CCSD/6-31+G(d)	CH_2=CLiCl	1.960	2.054	2.232	58.2
MIDIX	CH_2=CLiBr	1.955	2.271	2.322	63.4
		[1.915]	[2.313]	[2.279]	[66.3]
6-31G(d)	CH_2=CLiBr	1.967	2.174	2.366	59.4
		[1.951]	[2.287]	[2.309]	[64.3]
6-31+G(d)	CH_2=CLiBr	1.963	2.155	2.409	58.0
		[1.945]	[2.271]	[2.350]	[63.0]
6-31++G(d,p)	CH_2=CLiBr	1.964	2.148	2.413	57.7
		[1.945]	[2.272]	[2.350]	[63.0]
6-311++G(d,p)	CH_2=CLiBr	1.946	2.121	2.383	57.6
		[1.934]	[2.325]	[2.326]	[65.4]
aug-cc-pvdz	CH_2=CLiBr	1.967	2.123	2.464	55.0
aug-cc-pvtz	CH_2=CLiBr	1.946	2.084	2.402	56.1
CCSD/6-31+G(d)	CH_2=CLiBr	1.970	2.261	2.377	61.8

Table 5. Optimized MP2 [B3LYP] Bond Lengths (Å) and Angles (degrees) for the Planar Halovinyllithium Dimers **5**

Basis set	Molecule	C–Li	C–X	Li–X	θ C–Li–X
MIDIX	CH_2=CLiF	2.099	1.490	1.724	151.3
		[2.065]	[1.493]	[1.716]	[153.4]
6-31G(d)	CH_2=CLiF	2.125	1.520	1.774	151.9
		[2.096]$^{a)}$	[1.525]	[1.752]	[151.6]
6-31+G(d)	CH_2=CLiF	2.118	1.533	1.795	152.4
		[2.087]	[1.539]	[1.772]	[153.4]
6-31++G(d,p)	CH_2=CLiF	2.119	1.530	1.796	152.3
		[2.088]	[1.539]	[1.772]	[153.4]
6-311++G(d,p)	CH_2=CLiF	2.112	1.503	1.810	152.8
		[2.087]	[1.538]	[1.785]	[153.5]
aug-cc-pvdz	CH_2=CLiF	2.129	1.534	1.809	152.3
aug-cc-pvtz	CH_2=CLiF	2.119	1.494	1.819	153.4
CCSD/6-31+G(d)	CH_2=CLiF	2.109	1.538	1.779	151.0
MIDIX	CH_2=CLiCl	2.107	1.901	2.178	165.9
		[2.088]	[1.967]	[2.178]	[169.0]
6-31G(d)	CH_2=CLiCl	2.116	1.868	2.274	163.5
		[2.008]	[2.399]	[2.280]	[171.4]
6-31+G(d)	CH_2=CLiCl	2.112	1.864	2.262	163.9
		[2.002]	[2.371]	[2.266]	[169.8]
6-31++G(d,p)	CH_2=CLiCl	2.111	1.861	2.265	163.8
		[2.003]	[2.380]	[2.265]	[170.1]
6-311++G(d,p)	CH_2=CLiCl	2.115	1.857	2.231	164.3
		[2.005]	[2.415]	[2.257]	[173.3]
aug-cc-pvdz	CH_2=CLiCl	2.418	1.888	2.300	163.5
aug-cc-pvtz	CH_2=CLiCl	2.134	1.858	2.276	163.5
CCSD/6-31+G(d)	CH_2=CLiCl	2.114	1.892	2.253	164.7
MIDIX	CH_2=CLiBr	2.009	2.413	2.405	169.9
		[1.958]	[2.401]	[2.386]	[171.7]
6-31G(d)	CH_2=CLiBr	2.008	2.290	2.403	165.4
		[1.998]	[2.438]	[2.381]	[172.2]
6-31+G(d)	CH_2=CLiBr	1.994	2.176	2.433	157.8
		[1.985]	[2.402]	[2.411]	[170.7]
6-31++G(d,p)	CH_2=CLiBr	1.996	2.156	2.437	156.1
		[1.988]	[2.410]	[2.413]	[171.0]
6-311++G(d,p)	CH_2=CLiBr	2.124	2.023	2.400	166.8
		[1.992]	[2.486]	[2.424]	[174.2]
aug-cc-pvdz	CH_2=CLiBr	2.152	2.036	2.449	165.8
aug-cc-pvtz	CH_2=CLiBr	2.132	2.003	2.409	165.9
CCSD/6-31+G(d)	CH_2=CLiBr	2.067	2.745	2.410	179.5

a) A nearly planar chair structure was the stationary point at the B3LYP/6-31G(d) level.

basis set except the MIDIX. A similar trend was found for the C–Li–C bond angle of **3**. A larger range of C–Li–X bond angles was found in the dimer **2**, which is consistent with a relatively flat potential energy surface.

MP2 is often the highest practical level of theory that can be used for geometry optimizations of large molecules, and so it is instructive to compare the MP2/6-31+G(d) optimized geometries with those obtained by CCSD with the same basis set. The data in Tables 1–3 showed that the optimized C–Li and Li–X bond lengths were very similar between the two methods and that the CCSD optimizations generated slightly longer C–X bond lengths. These were still in the range of those obtained with the various basis sets at the MP2 or B3LYP levels. The MP2 and CCSD bond angles were also similar, and no major differences between the MP2 and CCSD optimized structures were observed.

A similar analysis was performed for the 1-halovinyllithium carbenoids, and the results are given in Tables 4–8. As with the halomethyllithiums, the dimer existed as two different constitutional isomers. The first of those is nominally C_2 symmetry, and exists in stable chair **6** and twist-boat **7** conformations, except for the fluoro-carbenoid, for which a stable twist-boat conformation was not found. A planar form **5** was slightly higher in energy than **6**, but one or two negative frequencies showed that it is not a minimum on the potential energy surface at the MP2 level. In contrast, the B3LYP calculations indicated that **5** was a local minimum with no negative frequencies. The other constitutional isomer was of approximately C_s symmetry for the fluoro carbenoid, and C_1 symmetry for the chloro- and bromocarbenoids **8**. Figure 2 shows the optimized geometries of the lithium vinylcarbenoids. The calculated bond lengths and angles of the 1-halovinyllithium monomer,

Table 6. Optimized MP2 [B3LYP] Bond Lengths (Å) and Angles (degrees) for the Chair Halovinyllithium Dimers **6**

Basis set	Molecule	C–Li	C–X	Li–X	θ C–Li–X
MIDIX	CH_2=CLiF	2.098[a)]	1.490	1.725	151.3
6-31G(d)	CH_2=CLiF	2.123	1.520	1.775	150.3
6-31+G(d)	CH_2=CLiF	2.119	1.533	1.802	148.7
6-31++G(d,p)	CH_2=CLiF	2.119	1.530	1.802	148.9
6-311++G(d,p)	CH_2=CLiF	2.114	1.503	1.815	148.9
aug-cc-pvdz	CH_2=CLiF	2.128	1.534	1.814	150.0
aug-cc-pvtz	CH_2=CLiF	2.119	1.495	1.821	151.1
CCSD/6-31+G(d)	CH_2=CLiF	2.110	1.538	1.781	148.0
MIDIX	CH_2=CLiCl	2.109	1.905	2.196	150.9
		[2.085]	[1.978]	[2.218]	[143.6]
6-31G(d)	CH_2=CLiCl	2.132	1.873	2.317	137.6
		[2.116]	[1.959]	[2.320]	[132.1]
6-31+G(d)	CH_2=CLiCl	2.124	1.868	2.300	142.9
		[2.108]	[1.952]	[2.303]	[136.8]
6-31++G(d,p)	CH_2=CLiCl	2.122	1.864	2.303	143.2
		[2.107]	[1.952]	[2.303]	[136.7]
6-311++G(d,p)	CH_2=CLiCl	2.119	1.862	2.266	141.1
		[2.117]	[1.956]	[2.270]	[138.9]
aug-cc-pvdz	CH_2=CLiCl	2.136	1.897	2.359	133.6
aug-cc-pvtz	CH_2=CLiCl	2.128	1.862	2.313	137.7
CCSD/6-31+G(d)	CH_2=CLiCl	2.120	1.897	2.289	143.1
MIDIX	CH_2=CLiBr	2.120	2.114	2.412	137.1
		[2.090]	[2.133]	[2.377]	[137.8]
6-31G(d)	CH_2=CLiBr	2.123	2.078	2.438	126.3
		[2.109]	[2.136]	[2.395]	[127.4]
6-31+G(d)	CH_2=CLiBr	2.110	2.057	2.528	120.7
		[2.091]	[2.112]	[2.482]	[121.7]
6-31++G(d,p)	CH_2=CLiBr	2.108	2.052	2.525	121.8
		[2.090]	[2.111]	[2.477]	[122.5]
6-311++G(d,p)	CH_2=CLiBr	2.125	2.033	2.456	136.3
		[2.121]	[2.130]	[2.438]	[134.2]
aug-cc-pvdz	CH_2=CLiBr	2.132	2.045	2.532	129.0
aug-cc-pvtz	CH_2=CLiBr	2.121	2.010	2.464	134.5
CCSD/6-31+G(d)	CH_2=CLiBr	2.109	2.100	2.506	120.9

a) CH_2=CLiF optimized only to the planar form at the B3LYP level. With the MIDIX basis set, the MP2 geometry was also planar.

planar, chair, and boat C_2 dimers, and C_s dimer are shown in Tables 4–7, respectively.

Overall, the basis set effects on 1-halovinyllithium carbenoid structures were similar to those on the halomethyllithium structures, with remarkable similarity between the 6-31+G(d) and 6-31++G(d,p) optimized geometries. Significantly different structures were obtained using the MIDIX basis set. Perhaps the most alarming fact was that the widely used B3LYP method incorrectly predicted the planar dimeric structure to be a local minimum and it failed to find a chair conformation for CH_2=CLiF. Comparison of the MP2 and CCSD optimized geometries showed trends similar to those with the halomethyllithium carbenoids. No significant structural changes were noted between the optimized geometries by the two methods, except for the planar form of the 1-bromovinyllithium dimer. In that case, the CCSD optimization resulted in a slight flattening of the 6-membered ring and a shorter Li–Li distance compared to the MP2 geometry, as illustrated in Fig. 3. No significant geometry change was observed with the analogous H_2C=CLiF and H_2C=CLiCl dimers.

Table 7. Optimized MP2 [B3LYP] Bond Lengths (Å) and Angles (degrees) for the Twist-Boat Halovinyllithium Dimers **7**

Basis set	Molecule	C–Li	C–X	Li–X	θ C–Li–X
MIDIX	CH_2=CLiCl	2.107	1.904	2.188	157.3
		[2.086]	[1.975]	[2.206]	[152.1]
6-31G(d)	CH_2=CLiCl	2.132	1.874	2.314	140.3
		[2.119]	[1.957]	[2.306]	[137.8]
6-31+G(d)	CH_2=CLiCl	2.122	1.868	2.299	145.1
		[2.107]	{1.950]	[2.292]	[143.2]
6-31++G(d,p)	CH_2=CLiCl	2.122	1.864	2.299	146.1
		[2.108]	[1.951]	[2.291]	[143.3]
6-311++G(d,p)	CH_2=CLiCl	2.121	1.862	2.265	140.8
		[2.120]	[1.953]	[2.262]	[144.2]
aug-cc-pvdz	CH_2=CLiCl	2.135	1.895	2.352	135.2
aug-cc-pvtz	CH_2=CLiCl	2.128	1.862	2.313	136.3
CCSD/6-31+G(d)	CH_2=CLiCl	2.119	1.897	2.286	147.2
MIDIX	CH_2=CLiBr	2.121	2.113	2.403	145.3
		[2.089]	[2.130]	[2.372]	[146.9]
6-31G(d)	CH_2=CLiBr	2.120	2.076	2.428	132.1
		[2.106]	[2.131]	[2.382]	[136.7]
6-31+G(d)	CH_2=CLiBr	2.110	2.054	2.482	128.8
		[2.092]	[2.107]	[2.442]	[135.5]
6-31++G(d,p)	CH_2=CLiBr	2.108	2.048	2.483	127.5
		[2.087]	[2.105]	[2.440]	[135.1]
6-311++G(d,p)	CH_2=CLiBr	2.127	2.030	2.453	136.0
		[2.123]	[2.123]	[2.427]	[142.2]
aug-cc-pvdz	CH_2=CLiBr	2.131	2.044	2.516	132.7
aug-cc-pvtz	CH_2=CLiBr	2.124	2.009	2.457	133.1
CCSD/6-31+G(d)	CH_2=CLiBr	2.107	2.095	2.462	132.8

Basis Set and Correlation Effects on Dimerization Energies. The data in Table 9 show the effect of the basis set on the dimerization of fluoromethyllithium. With both the B3LYP and MP2 methods, all basis sets predicted dimer **2** to be energetically favored over dimer **3** by about 1–2 kcal mol^{-1}. Furthermore, the B3LYP calculated dimerization free energies were all within about 2 kcal mol^{-1} of the MP2 calculated values. The smallest basis sets, that is, MIDIX and 6-31G(d), significantly overestimated the dimerization free energies. Starting from the 6-31+G(d) basis set, adding more polarization and diffuse functions had only a slight effect on the dimerization energies at the MP2 level, and up to about 2 kcal mol^{-1} at the B3LYP level. The G3 methods, the CCSD(T), and the large basis set MP2 calculations all generated dimerization free energies within about 1 kcal mol^{-1} of each other, except for the MP2/6-311++G(d,p). This suggests that further improvement is unlikely by going to higher levels of theory.

The basis set effects on the dimerization free energies of chloro- and bromomethyllithiums are shown in Tables 10 and 11, respectively. As with the fluorocarbenoid, both the B3LYP and MP2 methods calculated dimer **2** to be favored by 2–3 kcal mol^{-1} over dimer **3** with all basis sets except the 6-31G(d). At the MP2 level, the effects of adding more polarization and diffuse functions to the 6-31+G(d) basis set were minimal, and they were slightly larger at the B3LYP level. Use of the 6-311++G(2df,2pd), 6-311++G(3df,3pd), and the Dunning double and triple zeta basis sets resulted in lower

Table 8. Optimized MP2 [B3LYP] Bond Lengths (Å) and Angles (degrees) for the C_s Halovinyllithium Dimers **8**

Basis set	Molecule	C–Li	C–X	Li–X	θ C–Li–C
MIDIX	$\mathrm{CH_2{=}CLiF}$	2.096	1.490	1.723	118.6
		[2.055]	[1.493]	[1.716]	[119.2]
6-31G(d)	$\mathrm{CH_2{=}CLiF}$	2.114	1.520	1.785	117.4
		[2.083]	[1.521]	[1.759]	[119.4]
6-31+G(d)	$\mathrm{CH_2{=}CLiF}$	2.108	1.530	1.813	117.6
		[2.073]	[1.535]	[1.778]	[120.8]
6-31++G(d,p)	$\mathrm{CH_2{=}CLiF}$	2.109	1.528	1.812	117.6
		[2.072]	[1.536]	[1.777]	[121.0]
6-311++G(d,p)	$\mathrm{CH_2{=}CLiF}$	2.107	1.500	1.818	116.8
		[2.073]	[1.534]	[1.791]	[120.4]
aug-cc-pvdz	$\mathrm{CH_2{=}CLiF}$	2.116	1.532	1.816	117.9
aug-cc-pvtz	$\mathrm{CH_2{=}CLiF}$	2.106	1.493	1.828	116.2
CCSD/6-31+G(d)	$\mathrm{CH_2{=}CLiF}$	2.101	1.535	1.793	119.0
MIDIX	$\mathrm{CH_2{=}CLiCl}$	2.093	1.908	2.203	117.1
		[2.050]	[1.979]	[2.230]	[117.0]
6-31G(d)	$\mathrm{CH_2{=}CLiCl}$	2.121	1.870	2.324	113.8
		[2.083]	[1.958]	[2.340]	[115.4]
6-31+G(d)	$\mathrm{CH_2{=}CLiCl}$	2.112	1.864	2.309	114.8
		[2.076]	[1.947]	[2.327]	[116.3]
6-31++G(d,p)	$\mathrm{CH_2{=}CLiCl}$	2.112	1.860	2.310	114.9
		[2.076]	[1.948]	[2.325]	[116.4]
6-311++G(d,p)	$\mathrm{CH_2{=}CLiCl}$	2.103	1.858	2.273	114.5
		[2.076]	[1.947]	[2.296]	[116.5]
aug-cc-pvdz	$\mathrm{CH_2{=}CLiCl}$	2.117	1.896	2.371	114.4
aug-cc-pvtz	$\mathrm{CH_2{=}CLiCl}$	2.105	1.862	2.331	114.3
CCSD/6-31+G(d)	$\mathrm{CH_2{=}CLiCl}$	2.105	1.892	2.302	115.7
MIDIX	$\mathrm{CH_2{=}CLiBr}$	2.088	2.121	2.428	116.2
		[2.045]	[2.138]	[2.404]	[116.9]
6-31G(d)	$\mathrm{CH_2{=}CLiBr}$	2.111	2.081	2.407	113.7
		[2.079]	[2.136]	[2.381]	[116.4]
6-31+G(d)	$\mathrm{CH_2{=}CLiBr}$	2.090	2.061	2.491	113.6
		[2.060]	[2.115]	[2.471]	[115.6]
6-31++G(d,p)	$\mathrm{CH_2{=}CLiBr}$	2.091	2.057	2.484	113.6
		[2.058]	[2.116]	[2.462]	[115.9]
6-311++G(d,p)	$\mathrm{CH_2{=}CLiBr}$	2.102	2.027	2.472	114.3
		[2.072]	[2.123]	[2.481]	[116.0]
aug-cc-pvdz	$\mathrm{CH_2{=}CLiBr}$	2.113	2.047	2.539	113.6
aug-cc-pvtz	$\mathrm{CH_2{=}CLiBr}$	2.101	2.090	2.474	113.8
CCSD/6-31+G(d)	$\mathrm{CH_2{=}CLiBr}$	2.083	2.106	2.472	114.8

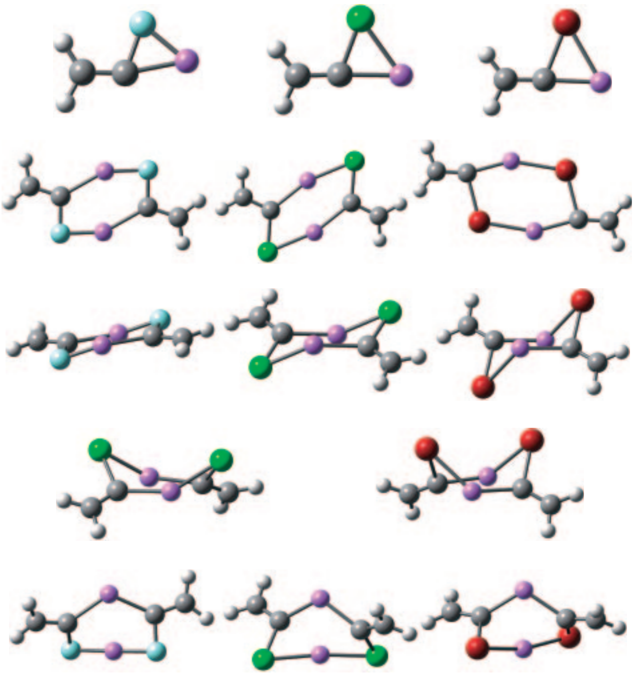

Fig. 2. Optimized geometries of halovinyllithium carbenoids. Top row: monomer **4**; second row: dimer **5**; third row: dimer **6**; fourth row: dimer **7**; bottom row: dimer **8**.

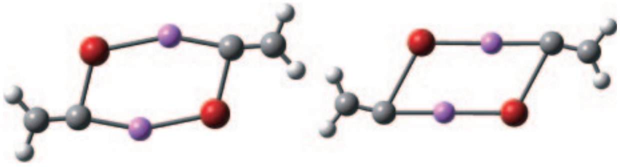

Fig. 3. Optimized geometries of the planar geometry of $\mathrm{H_2C{=}CLiBr}$ dimer. Left: MP2/6-31+G(d); Right: CCSD/6-31+G(d).

dimerization free energies by 3–4 kcal mol^{-1}, as did the G3 methods with chloromethyllithium. As with fluoromethyllithium, the G3, coupled cluster, and large basis set MP2 calculations differed from each other by only about 1–2 kcal mol^{-1} in the calculated dimerization free energies, suggesting that significant further improvement is unlikely to be attainable at a reasonable computational cost.

The dimerization free energies of 1-fluorovinyllithium are shown in Table 12. The potential energy surface of this compound was rather flat, and the relative free energies of the dimers were rather sensitive to the level of theory. At the MP2 level, two minima were found, corresponding to dimers **6** and **8**. Planar dimer **5** was not a minimum at the MP2 level, having one or two imaginary frequencies, and except for dimer **8**, was the only stable conformation of the dimer at the B3LYP level. The twist-boat conformation of the dimer **7** was not found for 1-fluorovinyllithium. The MP2 and coupled cluster calculations all predicted dimer **6** to be energetically favored over dimer **8** by up to 1.0 kcal mol^{-1}, whereas the G3 methods predicted dimer **8** to be the most stable form. This is likely do to the first step of the G3 calculation optimizing to an incorrect initial geometry of **6** during the Hartree–Fock (or B3LYP for G3B3) optimization step. As with the halomethyllithium carbenoids, the coupled cluster and large basis set MP2 calculations generated dimerization free energies that were very close to each other.

The dimerization free energies for 1-chloro- and 1-bromovinyllithiums are given in Tables 13 and 14, respectively. For both compounds, planar **5**, chair **6**, and twist-boat **7**, as well as isomer **8** were local minima, however, **5** had one or two imaginary frequencies at the MP2 level with all basis sets. At the B3LYP level, **5** and **6** were close in energy, and the lowest energy conformation varied with the basis set. In contrast, **6** was always the lowest energy form at the MP2 level. For the 1-chlorovinyllithium monomer, attempted G3 and G3MP2 calculations optimized toward an incorrect linear geometry in the first Hartree–Fock optimization step, which was confirmed by performing a Hartree–Fock re-optimization of the MP2 geometry. Thus, only the G3B3 dimerization energies was obtained

Table 9. Basis Set and Correlation Effects on the Dimerization Free Energies of $LiCH_2F$

Method	Basis Set	ΔG_f Dimer **2** /kcal mol^{-1}	ΔG_f Dimer **3** /kcal mol^{-1}
B3LYP	MIDIX	−49.1	−47.8
B3LYP	6-31G(d)	−38.7	−37.9
B3LYP	6-31+G(d)	−34.3	−33.7
B3LYP	6-31+G(d,p)	−34.1	−33.6
B3LYP	6-31++G(d,p)	−34.3	−33.7
B3LYP	6-311++G(d,p)	−32.2	−31.6
B3LYP	6-311++G(df,pd)	−32.7	−32.0
B3LYP	6-311++G(2df,2pd)	−32.2	−31.5
B3LYP	6-311++G(3df,3pd)	−32.2	−31.5
MP2	MIDIX	−48.9	−47.8
MP2	6-31G(d)	−40.4	−39.5
MP2	6-31+G(d)	−35.7	−34.9
MP2	6-31+G(d,p)	−35.4	−34.7
MP2	6-31++G(d,p)	−35.5	−34.8
MP2	6-311++G(d,p)	−35.1	−34.4
MP2	6-311++G(df,pd)	−36.7	−36.0
MP2	6-311++G(2df,2pd)	−34.2	−33.3
MP2	6-311++G(3df,3pd)	−33.9	−33.0
MP2	aug-cc-pvdz	−34.3	−33.8
MP2	aug-cc-pvtz	−33.6	−32.9
CCSD(T)//MP2	aug-cc-pvdz	−34.4	−33.9
G3	N/A	−34.9	−34.7
G3MP2	N/A	−34.5	−34.1
G3B3	N/A	−34.4	−34.0

Table 10. Basis Set and Correlation Effects on the Dimerization Free Energies of $LiCH_2Cl$

Method	Basis Set	ΔG_f Dimer **2** /kcal mol^{-1}	ΔG_f Dimer **3** /kcal mol^{-1}
B3LYP	MIDIX	−39.1	−36.2
B3LYP	6-31G(d)	−30.4	−26.5
B3LYP	6-31+G(d)	−27.5	−25.3
B3LYP	6-31+G(d,p)	−27.4	−25.2
B3LYP	6-31++G(d,p)	−27.7	−25.4
B3LYP	6-311++G(d,p)	−26.7	−24.0
B3LYP	6-311++G(df,pd)	−26.9	−24.2
B3LYP	6-311++G(2df,2pd)	−26.6	−24.0
B3LYP	6-311++G(3df,3pd)	−26.9	−24.1
MP2	MIDIX	−42.2	−40.3
MP2	6-31G(d)	−40.2	−32.0
MP2	6-31+G(d)	−33.3	−31.2
MP2	6-31+G(d,p)	−32.7	−31.1
MP2	6-31++G(d,p)	−33.3	−31.3
MP2	6-311++G(d,p)	−32.3	−30.5
MP2	6-311++G(df,pd)	−35.0	−33.1
MP2	6-311++G(2df,2pd)	−29.2	−27.2
MP2	6-311++G(3df,3pd)	−29.1	−27.2
MP2	aug-cc-pvdz	−29.7	−27.8
MP2	aug-cc-pvtz	−28.8	−26.8
CCSD(T)//MP2	aug-cc-pvdz	−29.4	−27.4
G3	N/A	−30.9	−28.0
G3MP2	N/A	−29.6	−26.7
G3B3	N/A	−31.4	−28.0

Table 11. Basis Set and Correlation Effects on the Dimerization Free Energies of $LiCH_2Br$

Method	Basis Set	ΔG_f Dimer **2** /kcal mol^{-1}	ΔG_f Dimer **3** /kcal mol^{-1}
B3LYP	MIDIX	−37.6	−33.8
B3LYP	6-31G(d)	−31.7	−30.3
B3LYP	6-31+G(d)	−28.1	−26.9
B3LYP	6-31+G(d,p)	−28.0	−26.8
B3LYP	6-31++G(d,p)	−28.4	−27.0
B3LYP	6-311++G(d,p)	−24.6	−21.5
B3LYP	6-311++G(df,pd)	−25.2	−22.1
B3LYP	6-311++G(2df,2pd)	−24.7	−21.8
B3LYP	6-311++G(3df,3pd)	−24.2	−21.5
MP2	MIDIX	−36.2	−33.2
MP2	6-31G(d)	−34.8	−34.1
MP2	6-31+G(d)	−31.3	−30.8
MP2	6-31+G(d,p)	−31.2	−30.7
MP2	6-31++G(d,p)	−31.7	−30.9
MP2	6-311++G(d,p)	−30.0	−27.9
MP2	6-311++G(df,pd)	−31.8	−29.7
MP2	6-311++G(2df,2pd)	−28.1	−26.3
MP2	6-311++G(3df,3pd)	−27.9	−26.1
MP2	aug-cc-pvdz	−29.0	−27.6
MP2	aug-cc-pvtz	−29.4	−27.4
CCSD(T)//MP2	aug-cc-pvdz	−28.6	−27.1

for 1-chlorovinyllithium. The coupled cluster, G3B3 and large basis set MP2 calculations were all within 1 kcal mol^{-1} of each other for 1-chlorovinyllithium. The 1-bromovinyllithium dimerization free energies were within about 2 kcal mol^{-1} of each other at the highest levels of theory, except for the planar conformer **5**, for which the coupled cluster dimerization energy was lower than the MP2 energy by about 3 kcal mol^{-1}.

These calculations show that, although the B3LYP method generally gives good geometries and energies for ground state organolithium molecules, it can generate erroneous results when the potential energy surface is rather flat. In this case, **5** is a second order saddle point which is only slightly higher in energy than the local minima, and that was mistaken for a local minimum by the B3LYP method.

Basis Set Effects on Thermal Corrections to Free Energies. Frequency calculations can become prohibitively expensive with large basis sets for even moderately sized molecules. A common solution to this problem is to perform a geometry optimization and frequency calculation with a smaller basis set, followed by re-optimization with a large basis set. The implicit assumption is that calculated corrections to the free energy are relatively insensitive to basis set effects and that, when calculating free energies of aggregation, the errors will tend to cancel. This hypothesis was tested by calculating the thermal correction for the free energy for the lithium carbenoid monomers and the most stable dimers, **2** and **6**, and tabulating the total thermal corrections to the dimerization free energies, as shown in Eqs. 1 and 2. The results are shown in Tables 15 and 16 for the halomethyllithium and 1-halovinyllithium carbenoids, respectively.

$$2 \text{ monomer } \mathbf{1} \rightarrow \text{dimer } \mathbf{2}. \tag{1}$$

$$2 \text{ monomer } \mathbf{4} \rightarrow \text{dimer } \mathbf{6}. \tag{2}$$

Table 12. Basis Set and Correlation Effects on the Dimerization Free Energies of $CH_2{=}CLiF$

Method	Basis Set	ΔG_f Dimer **5**/kcal mol^{-1}	ΔG_f Dimer **6**/kcal mol^{-1}	ΔG_f Dimer **7**/kcal mol^{-1}	ΔG_f Dimer **8**/kcal mol^{-1}
B3LYP	MIDIX	−44.9	N/A	N/A	−44.8
B3LYP	6-31G(d)	−37.6	N/A	N/A	−37.3
B3LYP	6-31+G(d)	−33.4	N/A	N/A	−32.8
B3LYP	6-31+G(d,p)	−33.3	N/A	N/A	−32.7
B3LYP	6-31++G(d,p)	−33.3	N/A	N/A	−32.8
B3LYP	6-311++G(d,p)	−31.0	N/A	N/A	−30.4
B3LYP	6-311++G(df,pd)	−32.1	N/A	N/A	−31.5
B3LYP	6-311++G(2df,2pd)	−31.7	N/A	N/A	−31.2
B3LYP	6-311++G(3df,3pd)	−31.8	N/A	N/A	−31.2
MP2	MIDIX	−46.7	−46.7[a]	N/A	−46.3
MP2	6-31G(d)	−38.8	−40.2	N/A	−39.5
MP2	6-31+G(d)	−34.6	−35.2	N/A	−34.7
MP2	6-31+G(d,p)	−34.6	−35.2	N/A	−34.3
MP2	6-31++G(d,p)	−34.6	−35.3	N/A	−34.3
MP2	6-311++G(d,p)	−34.7	−35.2	N/A	−34.6
MP2	6-311++G(df,pd)	−37.3	−37.8	N/A	−37.2
MP2	6-311++G(2df,2pd)	−34.8	−35.1	N/A	−34.4
MP2	6-311++G(3df,3pd)	−34.3	−34.7	N/A	−33.7
MP2	aug-cc-pvdz	−34.4	−34.4	N/A	−33.7
MP2	aug-cc-pvtz	−33.2	−34.3	N/A	−33.1
CCSD(T)//MP2	aug-cc-pvdz	−34.2	−34.2	N/A	−33.4
G3	N/A	−35.3	−35.7	N/A	−36.5
G3MP2	N/A	−34.7	−35.1	N/A	−35.8
G3B3	N/A	−34.4	−34.7	N/A	−35.5

a) Dimer **6** optimized to a planar geometry with the MIDIX basis set.

Table 13. Basis Set and Correlation Effects on the Dimerization Free Energies of $CH_2{=}CLiCl$

Method	Basis Set	ΔG_f Dimer **5**/kcal mol^{-1}	ΔG_f Dimer **6**/kcal mol^{-1}	ΔG_f Dimer **7**/kcal mol^{-1}	ΔG_f Dimer **8**/kcal mol^{-1}
B3LYP	MIDIX	−27.6	−30.6	−30.1	−30.2
B3LYP	6-31G(d)	−22.3	−25.8	−24.6	−25.1
B3LYP	6-31+G(d)	−23.4	−23.4	−22.5	−22.6
B3LYP	6-31+G(d,p)	−23.5	−23.2	−22.3	−22.5
B3LYP	6-31++G(d,p)	−23.5	−23.4	−22.4	−22.5
B3LYP	6-311++G(d,p)	−22.1	−21.1	−20.2	−20.2
B3LYP	6-311++G(df,pd)	−21.9	−21.8	−21.0	−20.7
B3LYP	6-311++G(2df,2pd)	−21.7	−22.4	−21.6	−20.4
B3LYP	6-311++G(3df,3pd)	−21.4	−22.3	−21.7	−21.6
MP2	MIDIX	−34.9	−37.4	−37.3	−36.6
MP2	6-31G(d)	−30.5	−34.2	−33.3	−33.4
MP2	6-31+G(d)	−29.5	−32.6	−32.2	−31.7
MP2	6-31+G(d,p)	−29.6	−32.7	−31.9	−31.8
MP2	6-31++G(d,p)	−29.8	−32.7	−32.0	−31.8
MP2	6-311++G(d,p)	−29.4	−32.1	−31.3	−31.2
MP2	6-311++G(df,pd)	−32.7	−34.8	−33.9	−33.8
MP2	6-311++G(2df,2pd)	−27.3	−29.3	−28.7	−28.3
MP2	6-311++G(3df,3pd)	−27.2	−29.6	−28.8	−28.6
MP2	aug-cc-pvdz	−25.5	−29.7	−28.9	−29.0
MP2	aug-cc-pvtz	−25.4	−28.9	−28.1	−28.0
CCSD(T)//MP2	aug-cc-pvdz	−24.2	−28.5	−27.7	−27.8
G3B3	N/A	−25.9	−29.0	−28.5	−28.2

The data in Table 15 showed that for the halomethyllithium carbenoids, the basis set effect on the thermal correction to the free energies were small. At the MP2 level, going form the 6-31G(d) to the aug-cc-pvtz, the thermal corrections all fell within one kcal mol^{-1} of each other for the fluoro- and chlorocarbenoids, with a slightly wider range at the B3LYP level. The bromomethyllithium had a slightly larger range of thermal corrections. For qualitative work, the MIDIX thermal correc-

Table 14. Basis Set and Correlation Effects on the Dimerization Free Energies of $\mathrm{CH_2{=}CLiBr}$

Method	Basis Set	ΔG_f Dimer **5**/kcal mol^{-1}	ΔG_f Dimer **6**/kcal mol^{-1}	ΔG_f Dimer **7**/kcal mol^{-1}	ΔG_f Dimer **8**/kcal mol^{-1}
B3LYP	MIDIX	−21.8	−28.9	−27.9	−28.6
B3LYP	6-31G(d)	−29.0	−28.4	−27.6	−28.7
B3LYP	6-31+G(d)	−25.2	−27.0	−25.8	−26.9
B3LYP	6-31+G(d,p)	−25.3	−26.8	−25.6	−26.7
B3LYP	6-31++G(d,p)	−25.1	−27.0	−26.4	−26.9
B3LYP	6-311++G(d,p)	−19.2	−18.8	−17.6	−18.0
B3LYP	6-311++G(df,pd)	−19.1	−19.7	−18.6	−18.8
B3LYP	6-311++G(2df,2pd)	−19.5	−19.4	−18.5	−18.7
B3LYP	6-311++G(3df,3pd)	−18.9	−19.6	−18.1	−18.6
MP2	MIDIX	−23.8	−30.6	−29.8	−30.1
MP2	6-31G(d)	−29.3	−34.8	−34.5	−35.0
MP2	6-31+G(d)	−25.0	−33.9	−32.8	−33.6
MP2	6-31+G(d,p)	−24.8	−33.9	−32.9	−33.6
MP2	6-31++G(d,p)	−27.2	−34.0	−33.4	−34.1
MP2	6-311++G(d,p)	−25.4	−29.1	−28.2	−28.2
MP2	6-311++G(df,pd)	−28.2	−31.4	−30.5	−30.3
MP2	6-311++G(2df,2pd)	−25.0	−28.0	−27.2	−27.1
MP2	6-311++G(3df,3pd)	−24.5	−27.8	−26.9	−26.9
MP2	aug-cc-pvdz	−24.3	−29.8	−28.8	−29.3
MP2	aug-cc-pvtz	−25.0	−29.1	−28.3	−28.4
CCSD(T)//MP2	aug-cc-pvdz	−22.9	−28.5	−27.4	−28.0

Table 15. Effects of Basis Sets on the Thermal Correction to the Free Energy of Halomethyllithium Carbenoid Dimerization

Method	Basis set	$\mathrm{LiCH_2F}$ /kcal mol^{-1}	$\mathrm{LiCH_2Cl}$ /kcal mol^{-1}	$\mathrm{LiCH_2Br}$ /kcal mol^{-1}
B3LYP	MIDIX	12.8	12.8	12.4
B3LYP	6-31G(d)	11.9	10.3	12.4
B3LYP	6-31+G(d)	12.1	12.0	11.7
B3LYP	6-31+G(d,p)	12.0	12.0	11.7
B3LYP	6-31++G(d,p)	12.0	11.7	12.4
B3LYP	6-311++G(d,p)	11.7	11.3	11.1
MP2	MIDIX	12.5	12.8	12.4
MP2	6-31G(d)	12.3	11.8	13.1
MP2	6-31+G(d)	12.3	12.0	12.5
MP2	6-31+G(d,p)	12.1	12.4	12.4
MP2	6-31++G(d,p)	12.1	11.9	12.9
MP2	6-311++G(d,p)	11.7	11.9	11.5
MP2	aug-cc-pvdz	11.8	11.3	11.5
MP2	aug-cc-pvtz	11.5	11.4	11.2

Table 16. Effects of Basis Sets on the Thermal Correction to the Free Energy of 1-Halovinyllithium Carbenoid Dimerization

Method	Basis set	$\mathrm{CH_2{=}CLiF}$[a] /kcal mol^{-1}	$\mathrm{CH_2{=}CLiCl}$ /kcal mol^{-1}	$\mathrm{CH_2{=}CLiBr}$ /kcal mol^{-1}
B3LYP	MIDIX	12.1	12.9	12.7
B3LYP	6-31G(d)	11.2	13.0	11.9
B3LYP	6-31+G(d)	11.2	12.9	12.7
B3LYP	6-31+G(d,p)	11.3	12.9	12.7
B3LYP	6-31++G(d,p)	11.4	12.8	12.7
B3LYP	6-311++G(d,p)	11.1	13.0	12.8
MP2	MIDIX	11.7	12.5	12.7
MP2	6-31G(d)	10.6	12.2	11.1
MP2	6-31+G(d)	11.2	12.6	12.2
MP2	6-31+G(d,p)	11.2	12.5	12.2
MP2	6-31++G(d,p)	11.3	12.6	12.2
MP2	6-311++G(d,p)	11.4	12.8	12.6
MP2	aug-cc-pvdz	11.1	12.4	12.3
MP2	aug-cc-pvtz	11.2	12.1	12.0

a) B3LYP structure was planar; MP2 was a chair conformation.

tions were also acceptable, and at the MP2 level, were very close to those obtained with larger basis sets.

As shown in Table 16, even though the dimerization energies of 1-halovinyllithium carbenoids were sensitive to the level of theory, the thermal corrections were not. At the B3LYP level, each of the basis sets generated thermal corrections within 1 kcal mol^{-1} of each other. The thermal corrections were nearly as consistent at the MP2 level, except that the 6-31G(d) basis set generated a smaller energy correction for the 1-fluoro- and bromovinyllithiums. We, therefore, concluded that the common practice of performing frequency calculations at lower levels of theory, followed by geometry re-optimization at higher levels, generates acceptable thermal corrections to the free energy for this class of compound.

Conclusion

The optimized geometries of halomethyllithium carbenoids were relatively insensitive to basis set effects and the method of electron correlation. For fluoromethyllithium, the dimerization energies calculated with the B3LYP hybrid DFT method were within a few kilocalories/mole of those obtained by MP2 with the same basis sets. Larger differences between B3LYP and MP2 energies were found with chloro- and bromomethyllithiums. Addition of extra polarization and diffuse functions to the 6-31+G(d) basis set scarcely had a an effect on the calculated dimerization energies, but larger basis sets affected the dimerization energies by several kilocalories/mole, particularly for the chloro- and bromomethyllithium carbenoids.

The 1-halovinyllithium carbenoids were much more sensitive to the level of theory, with the B3LYP method incorrectly predicting the planar dimer to be the most stable conformation. The G3 and G3MP2 methods failed for 1-chlorovinyllithium as the initial Hartree–Fock optimization step generated an incorrect geometry for the monomer. As with the halomethyllithium carbenoids, the coupled cluster, large basis set MP2, and G3 methods (when available) all generated comparable dimerization free energies.

In contrast to the free energies of dimerization, the thermal correction to the dimerization free energies were relatively insensitive to the level of theory, and even small basis sets could be used to obtain good thermal corrections. Thus, expensive frequency calculations with large basis sets can be avoided by performing geometry optimizations and frequency calculations with smaller basis sets to obtain the thermal correction, which is added to the electronic energy obtained from reoptimization with a larger basis set.

This work was supported in part by NSF grant #INT-0454045. This research used resources of the National Energy Research Scientific Computing Center, which is supported by the Office of Science of the U.S. Department of Energy under Contract No. DE-AC03-76SF00098. Thanks to Bala Ramachandran of Louisiana Tech for helpful discussions.

Supporting Information

Tables of optimized geometries and energies of all compounds at the MP2/6-31+G(d) and B3LYP/6-31+G(d) levels. This material is available free of charge on the web at http://www.csj.jp/journals/bscj/.

References

1 P. v. R. Schleyer, *Pure Appl. Chem.* **1984**, *56*, 151.

2 C. Rohde, T. Clark, E. Kaufmann, P. v. R. Schleyer, *J. Chem. Soc., Chem. Commun.* **1982**, 882.

3 G. D. Graham, D. S. Marynick, W. N. Lipscomb, *J. Am. Chem. Soc.* **1980**, *102*, 4572.

4 G. D. Graham, S. Richtsmeier, D. A. Dixon, *J. Am. Chem. Soc.* **1980**, *102*, 5759.

5 F. E. Romesberg, D. B. Collum, *J. Am. Chem. Soc.* **1992**, *114*, 2112.

6 M. P. Bernstein, F. E. Romesberg, D. J. Fuller, A. T. Harrison, D. B. Collum, Q. Y. Liu, P. G. Williard, *J. Am. Chem. Soc.* **1992**, *114*, 5100.

7 F. E. Romesberg, D. B. Collum, *J. Am. Chem. Soc.* **1994**, *116*, 9187.

8 F. E. Romesberg, M. P. Bernstein, J. H. Gilchrist, A. T. Harrison, D. J. Fuller, D. B. Collum, *J. Am. Chem. Soc.* **1993**, *115*, 3475.

9 L. M. Pratt, N. V. Nguyễn, B. Ramachandran, *J. Org. Chem.* **2005**, *70*, 4279.

10 L. M. Pratt, N. V. Nguyễn, *J. Org. Chem.* **2005**, *70*, 10561.

11 E.-U. Würthwein, D. Hoppe, *J. Org. Chem.* **2005**, *70*, 4443.

12 F. Haeffner, K. N. Houk, S. M. Schulze, J. K. Lee, *J. Org. Chem.* **2003**, *68*, 2310.

13 E. Nakamura, S. Mori, K. Morokuma, *J. Am. Chem. Soc.* **1998**, *120*, 8273.

14 L. M. Pratt, B. Ramachandran, J. D. Xidos, C. J. Cramer, D. G. Truhlar, *J. Org. Chem.* **2002**, *67*, 7607.

15 L. M. Pratt, B. Ramachandran, *J. Org. Chem.* **2005**, *70*, 7238.

16 L. M. Pratt, L. T. Lê, T. N. Truong, *J. Org. Chem.* **2005**, *70*, 8298.

17 L. M. Pratt, N. V. Nguyễn, L. T. Lê, *J. Org. Chem.* **2005**, *70*, 2294.

18 M. J. Frisch, G. W. Trucks, H. B. Schlegel, G. E. Scuseria, M. A. Robb, J. R. Cheeseman, J. A. Montgomery, Jr., T. Vreven, K. N. Kudin, J. C. Burant, J. M. Millam, S. S. Iyengar, J. Tomasi, V. Barone, B. Mennucci, M. Cossi, G. Scalmani, N. Rega, G. A. Petersson, H. Nakatsuji, M. Hada, M. Ehara, K. Toyota, R. Fukuda, J. Hasegawa, M. Ishida, T. Nakajima, Y. Honda, O. Kitao, H. Nakai, M. Klene, X. Li, J. E. Knox, H. P. Hratchian, J. B. Cross, C. Adamo, J. Jaramillo, R. Gomperts, R. E. Stratmann, O. Yazyev, A. J. Austin, R. Cammi, C. Pomelli, J. W. Ochterski, P. Y. Ayala, K. Morokuma, G. A. Voth, P. Salvador, J. J. Dannenberg, V. G. Zakrzewski, S. Dapprich, A. D. Daniels, M. C. Strain, O. Farkas, D. K. Malick, A. D. Rabuck, K. Raghavachari, J. B. Foresman, J. V. Ortiz, Q. Cui, A. G. Baboul, S. Clifford, J. Cioslowski, B. B. Stefanov, G. Liu, A. Liashenko, P. Piskortz, I. Komaromi, R. L. Martin, D. J. Fox, T. Keith, M. A. Al-Laham, C. Y. Peng, A. Nanayakkara, M. Challacombe, P. M. W. Gill, B. Johnson, W. Chen, M. W. Wong, C. Gonzalez, J. A. Pople, *Gaussian 03, Revision A.1*, Gaussian, Inc., Pittsburgh, PA, **2003**.